# Numerical Simulation of Interacting Magnetic Flux Ropes

Dusan Odstrcil[*], Marek Vandas[†], Victor J. Pizzo[**] and Peter MacNeice[‡]

[*]*University of Colorado, CIRES-NOAA/SEC, 325 Broadway, Boulder, Colorado 80305, USA*
[†]*Astronomical Institute, Academy of Sciences, Boční II 1401, 14131 Praha, Czech Republic*
[**]*NOAA/Space Environment Center, 325 Broadway, Boulder, Colorado 80305, USA*
[‡]*Drexel University, NASA/GSFC, Greenbelt, Maryland 20771, USA*

**Abstract.** A $2\frac{1}{2}$-D MHD numerical model is used to investigate the dynamic interaction between two flux ropes (clouds) in a homogeneous magnetized plasma. One cloud is set into motion while the other is initially at rest. The moving cloud generates a shock which interacts with the second cloud. Two cases with different characteristic speeds within the second cloud are presented. The shock front is significantly distorted when it propagates faster (slower) in the cloud with larger (smaller) characteristic speed. Correspondingly, the density behind the shock front becomes smaller (larger). Later, the clouds approach each other and by a momentum exchange they come to a common speed. The oppositely directed magnetic fields are pushed together, a driven magnetic reconnection takes a place, and the two flux ropes gradually coalescence into a single flux rope.

## INTRODUCTION

Coronal mass ejections (CMEs) represent a major transient release of mass and energy from the Sun. Recently, evidence of interacting CMEs was found in radio observations [1]. In this paper, we will investigate the dynamic interaction between two magnetic flux ropes using numerical magnetohydrodynamic (MHD) simulation. The aim is to provide some qualitative picture of the shock-cloud and cloud-cloud interactions.

## NUMERICAL SIMULATIONS

The $2\frac{1}{2}$-D ideal MHD equations are solved in Cartesian coordinates using an explicit, multi-dimensional version of the TVDLF scheme [2]. The Paramesh adaptive mesh refinement (AMR) package [3] is used to obtain high resolution of fine structures.

We consider the case of a moderate ambient magnetic field with $\beta = 4.8$ (where $\beta$ is the ratio of the thermal to magnetic pressure) with an adiabatic index $\gamma = 5/3$, initial temperature $T_0 = 3/5$, initial density $\rho_0 = 1$, and initial background magnetic field $B_0 = 0.5$. We use units where the gas constant and magnetic permeability are set to unity. Thus the sound velocity $C_0^S = (\gamma T_0)^{1/2} = 1$ and the Alfven velocity $C_0^A = |B_0|/\rho_0^{1/2} = 0.5$. Two magnetic flux ropes (clouds), left and right, are considered. The left cloud has the central field strength $B_L = 3 \times B_0$ and plasma density $\rho_L = 3 \times \rho_0$. The right cloud is specified with two different cases for its field strength and plasma density. Namely, $B_R = 4\times (2\times) B_0$ and $\rho_R = 2\times (4\times) \rho_0$ for Case 1 (2). The temperature is adjusted

to provide constant thermal pressure everywhere. The magnetic pressure in the right cloud is a factor 16 (4) larger than in the external medium and the minimum $\beta$ inside the cloud is 0.3 (1.2) in Case 1 (2).

Figure 1 shows the initial profile of various quantities for both cases. The density, temperature, and velocity are constant within the clouds. The magnetic field components follow Lundquist's force-free solution surrounded by a potential field. The clouds are initially cylindrical, the radius $R_L = R_R$ is set to unity, and this is chosen as the unit of length. The unit of time is set to the cloud sound crossing time $\tau = R_R/C_0^S$. Further, the flow velocity is expressed in units of the sound velocity. The rectangular domain of our simulation (-12.5 $\leq x \leq$ 12.5 and -12.5 $\leq y \leq$ 12.5) is chosen so that the boundaries are sufficiently far away from the clouds to avoid numerical artifacts. The center of the left cloud is located at $x = -7.5$ and $y = 0$. The center of the right cloud is located at $x = 0$ and $y = 0$. A maximum numerical resolution corresponds to a uniform grid with $512 \times 512$ computational cells. This gives a resolution of 20 zones per initial cloud radius, which is sufficient to capture basic cloud evolution.

## RESULTS AND DISCUSSION

At time $t = 0$ the left cloud is set initially into motion with velocity $V_L = 1.5 \times C_0^S$ parallel to the ambient magnetic field. This leads to the immediate formation of a shock pair at the right (leading) edge of the cloud and rarefaction waves at the left edge of the cloud. A forward shock propagates ahead of the cloud to the right and a reverse shock propagates through the cloud to the left. We
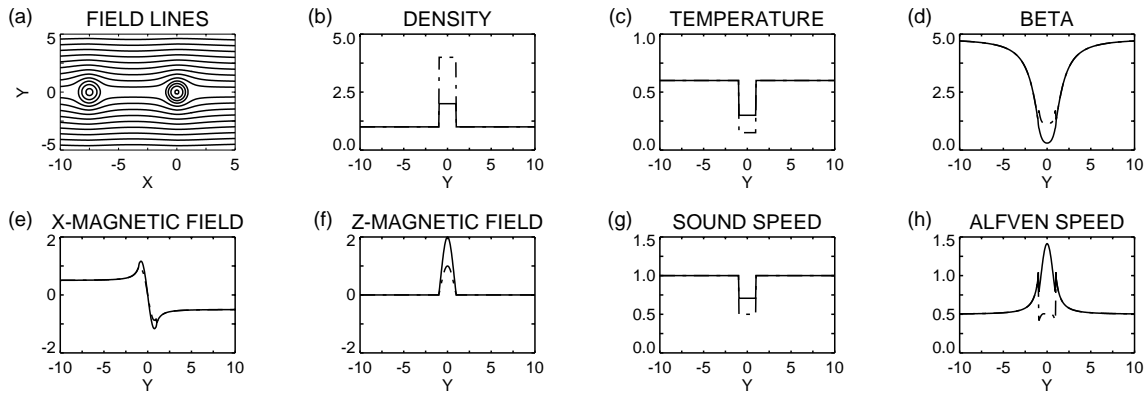
**FIGURE 1.** Initial conditions used for simulations of two interacting magnetic flux ropes. Two different cases with the same magnetic field topology (a) and parameters of the left cloud but differing parameters within the right cloud (b-h; profiles are through the cloud center, $x=0$) are considered in this paper. Case 1 (Case 2) has cloud parameters yielding larger (smaller) maximum characteristic speed than the background medium, as indicated by solid (dash-dot) line profiles.
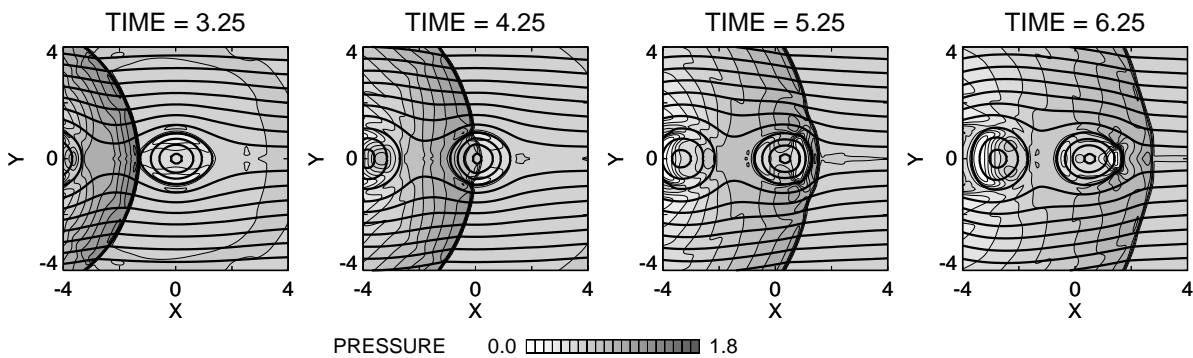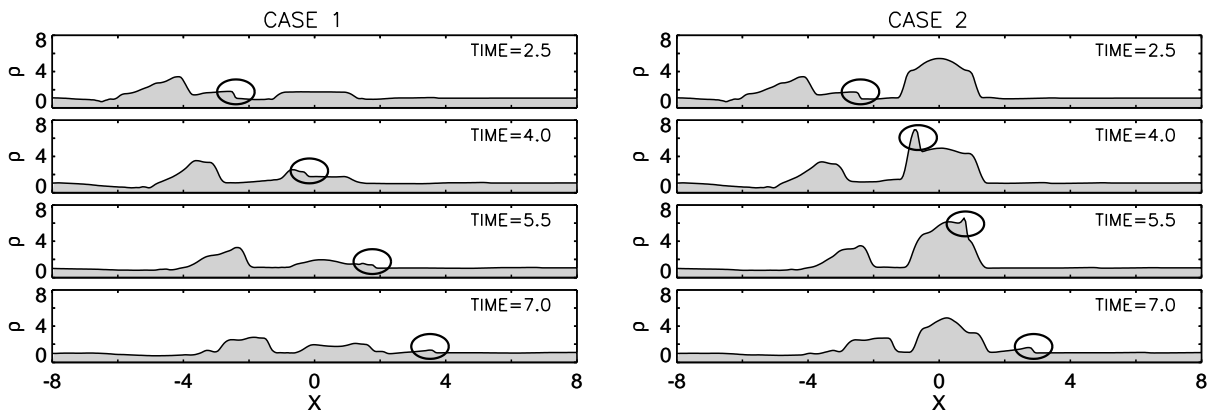


**FIGURE 2.** Interacting magnetic flux ropes for Case 1. Distribution of the thermal pressure (grey shading and light lines) and magnetic field lines (thick lines), is shown at four different times.
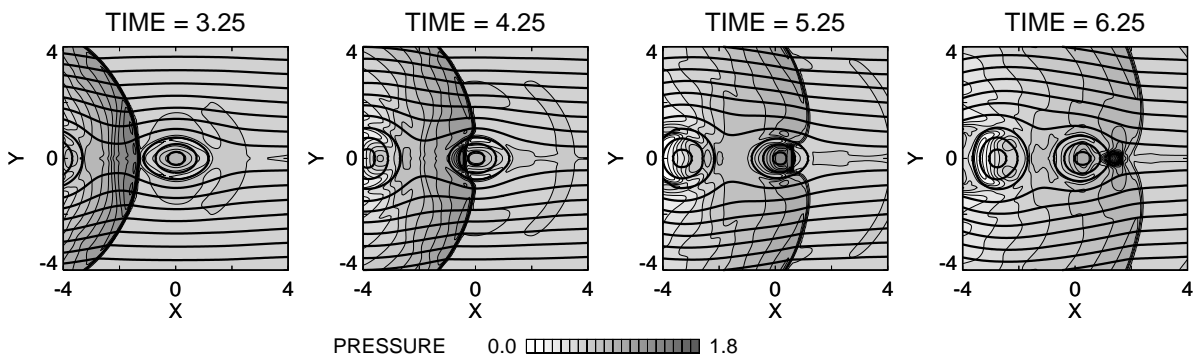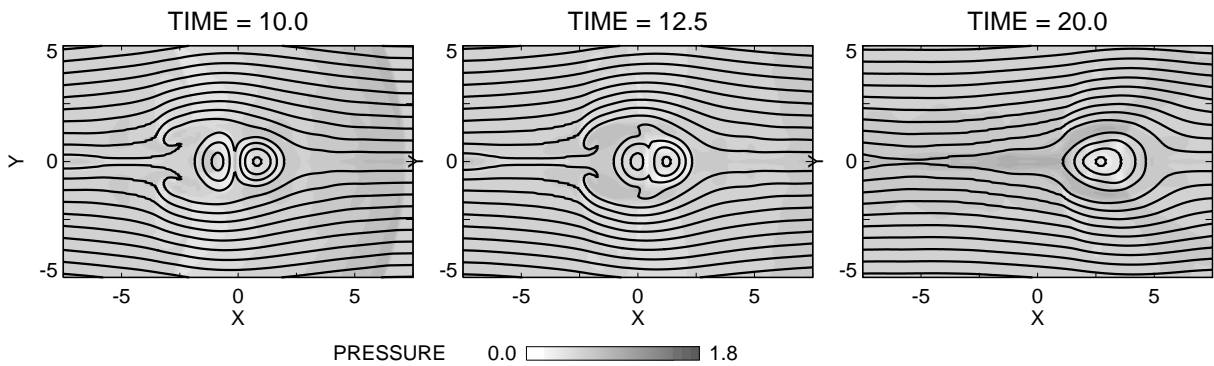


**FIGURE 3.** Interacting magnetic flux ropes for Case 2. Distribution of the thermal pressure (grey shading and light lines) and magnetic field lines (thick lines), is shown at four different times.
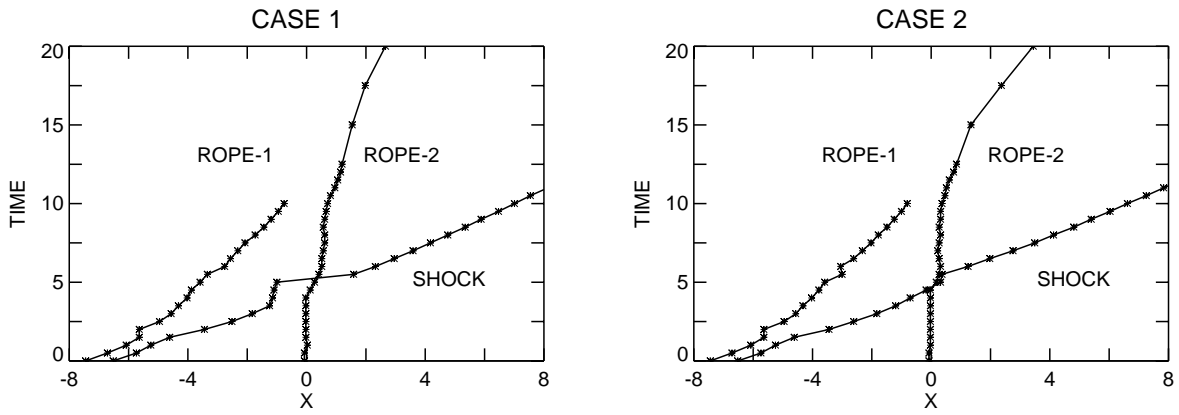
**FIGURE 4.** Trajectories of the magnetic flux rope centers (field strength maxima) and the shock (pressure maximum) for Case 1 (left panel) and Case 2 (right panel).



**FIGURE 5.** Density profiles through the magnetic flux rope centers ($y$=0) at four different times for Case 1 (left panel) and Case 2 (right panel). Positions of the shock are marked by a thick oval.



**FIGURE 6.** Interacting magnetic flux ropes for Case 1. Distribution of the thermal pressure (grey shading) and magnetic field lines (thick lines), is shown at three different times.

will discuss only the forward, "piston-driven", shock that forms in front of the left cloud and propagates toward the right cloud.

Figures 2 and 3 show the evolution of the dynamic interaction for Case 1 and Case 2, respectively. The left cloud generates a forward shock that starts to enter the right cloud at about $t = 3.25$. However, the differing parameters within the right cloud (see Fig. 1) cause differences during the shock-cloud interaction process. In Case 1, the larger characteristic speed causes faster shock propagation and concave-outward distortion of the shock front (Fig. 2). The shock leaves the cloud at about $t = 5.0$, visibly ahead of the shock portions that propagated through the surrounding medium. Since the shock is relatively weak, its effect on the cloud is weak as well. In Case 2, the lower characteristic speed causes slower shock propagation and concave-inward distortion of the shock front (Fig. 3). The shock leaves the cloud at about $t = 5.75$, significantly behind the shock portions that propagated through the surrounding medium. Effects on the cloud are larger due to the stronger shock. The magnetic structure is compressed and becomes oblate. Note that at larger times the shock fronts in both cases gradually acquire a uniform shape (after $t = 8$) and they "forget their history".

Figure 4 shows positions of the cloud centers and shocks as function of time for two different cases. When the shock enters the cloud, the momentum of the post-shock flow accelerates the cloud. This effect has been reported previously [4]. However, this acceleration is not permanent in our examples. Further, our results show that the shock can either accelerate or decelerate within the cloud depending on physical parameters within the cloud. Note that only shock acceleration was described in the interplanetary shock-cloud simulation [4].

Figure 5 shows the plasma density profiles through the cloud centers. The shock front is accelerated (decelerated) in the cloud with larger (smaller) characteristic speed. Correspondingly, the density behind the shock front becomes smaller (larger). This latter behavior is similar to ocean waves; as they approach the shallows near the coast, they slow down and their height increases.

Later, the clouds approach each other and in the subsequent momentum exchange they come to a common speed. Note that both flux ropes have the same rotation of the magnetic field, i.e., there are oppositely directed magnetic fields at the leading edge of the left cloud and at the trailing edge of the right cloud. These oppositely directed magnetic fields are pushed together and a driven magnetic reconnection takes a place. The reconnection process (caused by numerical diffusion) proceeds slowly and two flux ropes coalescence into a single flux rope gradually (Fig. 6).

## CONCLUSIONS

The shock-cloud and cloud-cloud interactions are rather complex and different parameters can produce different outcomes. We present only two cases here, each having the same background state, cloud shape, and cloud velocity, but with different clouds characteristic speeds. We have found that: (1) the shock front is significantly distorted because it propagates faster (slower) in the cloud with larger (smaller) characteristic speed; and (2) correspondingly, the density behind the shock front becomes smaller (larger). Later on, the clouds approach each other, with the results that: (1) the clouds acquire the same speed; (2) the oppositely directed magnetic fields are pushed together and driven magnetic reconnection takes a place; and (3) the two flux ropes gradually coalescence into a single flux rope. The parameters of the clouds and background state we have considered are quite ideal, and they provide only a qualitative picture of the true interaction of CMEs and shocks.

During the interaction all characteristic parameters of the initial structures are modified, and this may lead to observable effects in remote observations of the coronal white-light and radio-emission, as well as for in-situ observations of energetic particles, plasma parameters, and magnetic field. Specifically, patchy enhancements of type II radio bursts and apparently irregular changes in frequency drift rate may be associated with localized shock strengthening and distortion, shock acceleration or deceleration, and the generation of complex shock patterns and reflections. Further, shock-cloud and cloud-cloud interactions may enhance electron and ion acceleration and/or magnetic field reconnection processes that will affect energetic particles. Finally, such interactions between the Sun and Earth can: (1) modify parameters of a single transient disturbance (shock strength, momentum, southward magnetic field); (2) reduce the number of shocks and magnetic clouds by "cannibalism"; and (3) lead to compound events with extended durations. All these effects complicate space weather forecasting in ways that are yet poorly understood.

## REFERENCES

1. Gopalswamy, N., *Astrophys. J. Letts.* **548**, L91-L94 (2001).
2. Toth, G., and Odstrcil, D., *J. Comput. Phys.* **128**, 82-100 (1996).
3. MacNeice, P., Olson, K. M. Mobarry, C., Faichstein, de R., and Packer, C., *Comput. Phys. Commun.* **126**, 330-354 (2000).
4. Vandas, M., Fischer, S., Dryer, M., Smith, Z., and Detman, T., *J. Geophys. Res.* **102**, 22,295-22,300 (1997).